Intermediate-Temperature Reverse Water−Gas Shift under Process-Relevant Conditions Catalyzed by Dispersed Alkali Carbonates

Published as part of JACS Au special issue "Advances in Small Molecule Activation Towards Sustainable Chemical Transformations".

Kesha N. Tamakuwala, Robert P. Kennedy, Chastity S. Li, Benjamin Mutz, Peter Boller, Simon R. Bare, and Matthew W. Kanan*

Read Online

ACCESS | Metrics & More | Article Recommendations | SI Supporting Information

ABSTRACT: Current reverse water−gas shift (RWGS) technologies require extreme temperatures of >900 °C. The ability to perform RWGS at lower temperatures could open new opportunities for sustainable chemical and fuel production, but most catalyst materials produce methane and coke at lower temperatures, especially at elevated pressures targeted for industrial processes. Here we show that transition-metal-free catalysts composed of K_2CO_3 or Na_2CO_3 dispersed on commercial γ-Al_2O_3 supports (K_2CO_3/γ-Al_2O_3 and Na_2CO_3/γ-Al_2O_3) are highly effective RWGS catalysts in the intermediate-temperature regime. At a high gas hourly space velocity of 30,000 h^{-1} and operating pressure of 10 bar, K_2CO_3/γ-Al_2O_3 reached RWGS equilibrium-limited CO_2 conversion at 550 °C and was 100% selective for CO at all temperatures tested (up to 700 °C). Na_2CO_3/γ-Al_2O_3 was also 100% CO-selective and only slightly less active. Both catalysts were stable for hundreds of hours on stream at 525 °C and tolerated large quantities of methane and propane impurity in the CO_2/H_2 feed. The unique performance attributes, combined with the low-cost components and extremely simple synthesis, make dispersed carbonate RWGS catalysts attractive options for industrial application.

KEYWORDS: CO_2 hydrogenation, reverse water−gas shift, heterogeneous catalysis, dispersed carbonate catalyst, Syngas production, Power-to-liquid
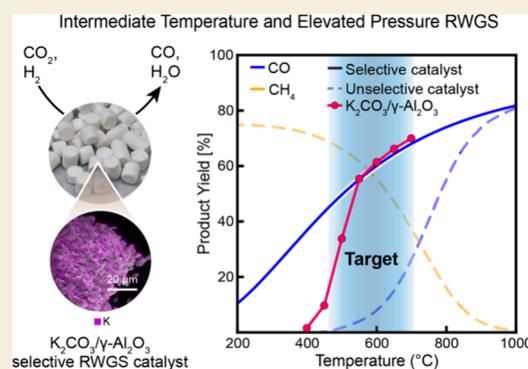
1. INTRODUCTION

Reverse water−gas shift (RWGS) catalysis is an essential component of emerging technologies to produce sustainable fuels and chemicals (Figure 1a). RWGS is used to synthesize the CO component of syngas (a mixture of CO and H_2), which can be converted into a variety of products by thermal or biological syngas conversion processes. Recently commercialized power-to-liquid (PtL) systems integrate water electrolysis to make renewable H_2, RWGS to convert H_2 and CO_2 into syngas, and Fischer−Tropsch catalysis to convert syngas into liquid hydrocarbons.[1−4] Alternatively, electrolysis and RWGS can be combined with gas fermentation to make ethanol.[5] Given the feedstock constraints and land use change concerns associated with biofuels,[6] large-scale PtL processes powered by renewable electricity may be needed to decarbonize hard-to-abate sectors such as aviation, heavy-duty trucks, and shipping, which presently consume >60 million barrels of oil per day.[7] Beyond fuels, RWGS enables a wide range of power-to-chemicals systems since CO and syngas are feedstocks for a significant portion of the chemical industry.[8] In addition to applications where H_2 is sourced from H_2O

electrolysis, RWGS can be used to increase the CO content of gasified biomass in systems that convert biomass into fuels or chemicals.[9]

Selectivity is arguably the most difficult challenge for RWGS catalysis. RWGS is an endothermic reaction (eq 1), but the competing methanation (Sabatier) reaction is strongly exothermic (eq 2).[10] At thermodynamic equilibrium between CO_2, H_2, CO, CH_4, and H_2O, CH_4 is the favored product until ∼700 °C and remains a significant product until temperatures >900 °C (Figure 1b). Thus, unselective CO_2 hydrogenation catalysts that catalyze both RWGS and methanation produce large amounts of CH_4 at less extreme temperatures. Additionally, catalysts can be deactivated by coke formation through
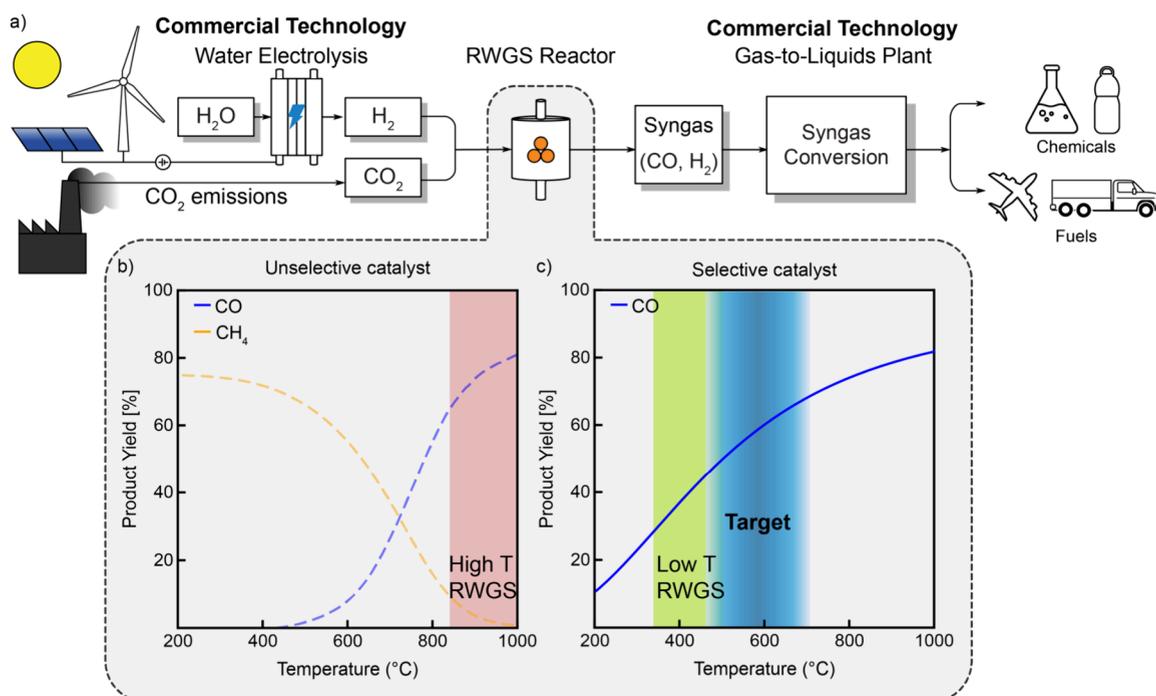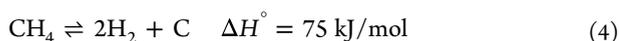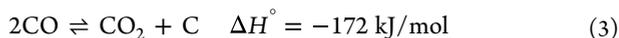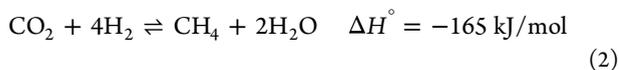
Figure 1. a) Schematic showing PtL process to make chemicals and fuels starting with electricity, H_2O, and CO_2 using RWGS reaction. Product yields at thermodynamic equilibrium for 3:1 H_2:CO_2 inlet feed at 10 bar with b) unselective and c) CO selective catalysts are indicated along with three temperature-regimes for RWGS catalysis.

either the exothermic Boudouard reaction (eq 3) or endothermic methane dehydrogenation (eq 4).[10]

$$CO_2 + H_2 \rightleftharpoons CO + H_2O \quad \Delta H^\circ = 41 \text{ kJ/mol} \quad (1)$$

$$CO_2 + 4H_2 \rightleftharpoons CH_4 + 2H_2O \quad \Delta H^\circ = -165 \text{ kJ/mol} \quad (2)$$

$$2CO \rightleftharpoons CO_2 + C \quad \Delta H^\circ = -172 \text{ kJ/mol} \quad (3)$$

$$CH_4 \rightleftharpoons 2H_2 + C \quad \Delta H^\circ = 75 \text{ kJ/mol} \quad (4)$$

Commercial RWGS technologies utilize unselective Ni-based catalysts that are typically operated at >850 °C to suppress CH_4 and avoid coking.[1,3,11] Such extreme temperatures necessitate the use of expensive, thick-walled reactors and can complicate heat integration with downstream syngas-to-liquid conversion processes, which operate at much lower temperatures (e.g., <350 °C for FT[12] and <70 °C for gas fermentation[13]). As a potential alternative to Ni catalysts, Cu/ZnO-based catalysts are highly active and selective for RWGS in the low temperature range (<500 °C),[14] but have poor stability at higher temperatures.[15] Ni on silicalite-1[16] and molten-salt-prepared K,Na–Ni/SiO$_2$[17] have shown similarly high activity and CO selectivity in this low-temperature range but have not been tested at higher temperatures. Operating at low temperatures results in low equilibrium-limited CO yields (Figure 1b), which may necessitate costly separations. Moreover, the limited stability window places restrictions on reactor design. It is problematic to use adiabatic reactors, since they require a high inlet gas temperature to provide the heat for the endotherm.

Selective RWGS catalysis in the intermediate temperature range (ca. 500 to 700 °C) is a highly attractive target because it enables relatively high CO yield without the challenges of managing and integrating extreme temperatures (Figure 1c).

However, this regime is the most challenging from a selectivity perspective because the competing methanation and coking reactions are still thermodynamically favored and there is substantial thermal energy available to overcome activation barriers to these undesired pathways.

In addition to temperature considerations, it is important for RWGS catalysts to accommodate elevated pressure. The inputs to RWGS are likely to be delivered at pressure—CO_2 is transported at elevated pressure and pressurized H_2 is generated directly by commercial water electrolyzers (e.g., 30–40 bar for PEM systems[18]). Downstream of RWGS, FT reactors operate at pressures of 20–45 bar[19] and gas fermentation requires elevated pressure to increase gas–liquid mass transport.[20] Operating RWGS at elevated pressure is beneficial to the reaction kinetics and can improve overall process efficiency by avoiding unnecessary compression/decompression losses.[21] However, both methanation and coke formation via the Boudouard reaction are favored as pressure is increased because these reactions result in net consumption of gas molecules. Thus, increased pressure exacerbates the selectivity challenge for intermediate-temperature RWGS catalysis.

Recent reports have described a few transition metal-based catalysts that exhibit promising RWGS selectivity at intermediate temperatures, yet these studies have been limited to 1 bar operating pressure. NiO on CeO$_2$[22] and FeCu on Al$_2$O$_3$–CeO$_2$[12] showed essentially 100% CO selectivity at 400 to 750 °C, although long-term stability has not been demonstrated for these catalysts. Catalysts composed of molybdenum phosphide and phosphate on SiO$_2$ (Mo–P/SiO$_2$) have reached 100% CO selectivity at 450–550 °C but form coke at higher temperatures.[23] Vanadium and molybdenum carbides have shown promising activity and selectivity at 1 bar,[24,25] with a recent report demonstrating 100% CO selectivity at 600 °C and no loss in activity for 500 h on stream
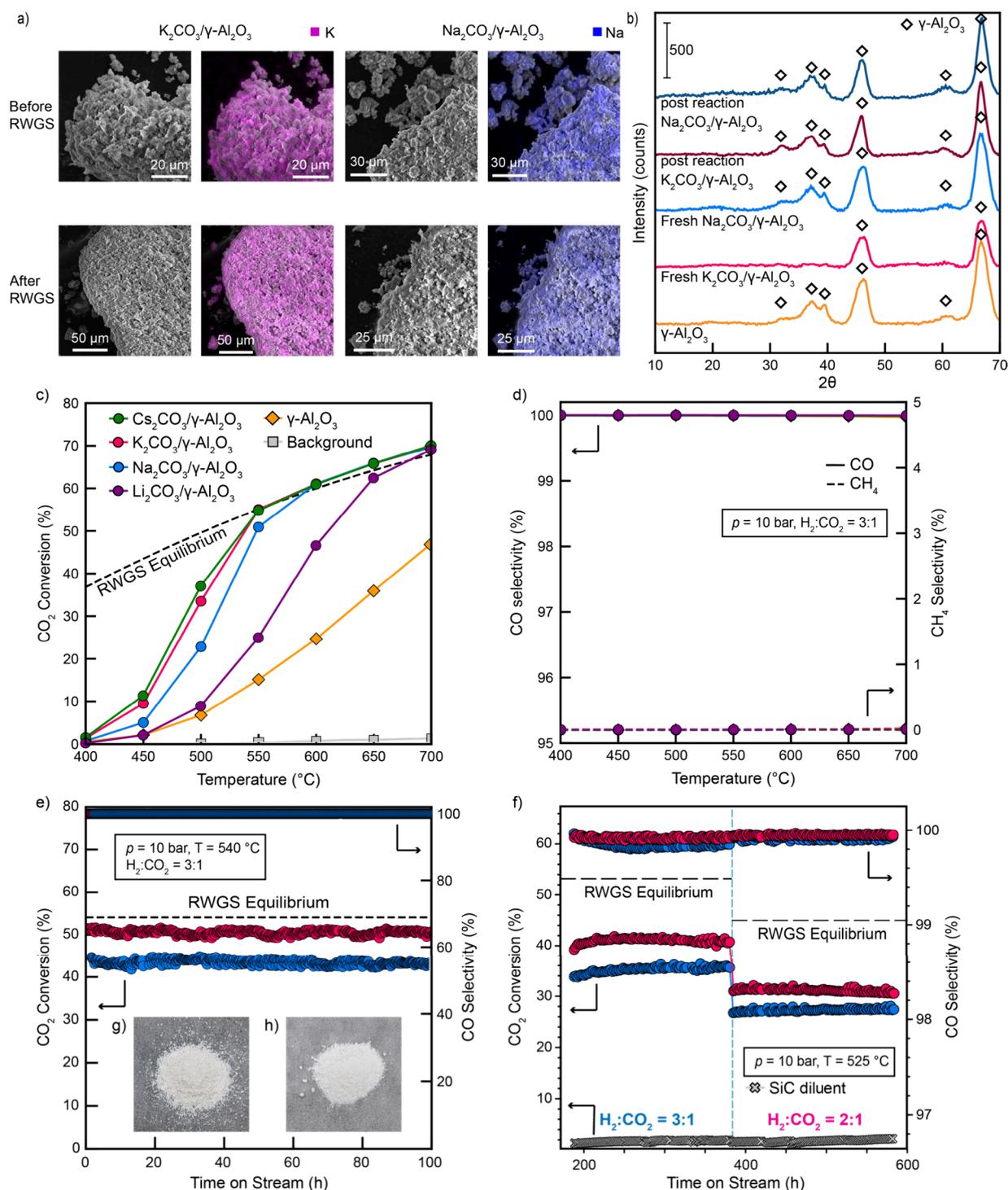
Figure 2. RWGS performance and catalyst characterization: a) SEM images and EDX mapping of alkali metals and b) Powder XRD patterns for freshly synthesized versus post-reaction K_2CO_3/γ-Al_2O_3 and Na_2CO_3/γ-Al_2O_3 catalysts. c) CO_2 conversion and d) CO selectivity versus temperature for dispersed carbonate catalysts, γ-Al_2O_3, and reactor background. e) CO_2 conversion and CO selectivity versus time on stream for carbonate catalysts with optical images of g) K_2CO_3/γ-Al_2O_3 and h) Na_2CO_3/γ-Al_2O_3 post reaction. f) CO_2 conversion and CO selectivity versus time on stream for extended durability testing of dispersed carbonate catalysts.

with a nanocrystalline α-Mo_2C catalyst.[26] While performance at elevated pressure was not reported for this α-Mo_2C catalyst, a related catalyst comprised of P- and K-doped Mo_2C on γ-Al_2O_3 evaluated at 20 bar showed good CO selectivity (>98%) and long-term stability at 450 °C but rapidly coked and switched to CH_4 as the dominant product at 600 °C.[27] Similarly, testing commercial Ni/Al_2O_3 and $Rh/CeO_2/Al_2O_3$

catalysts in the 550−850 °C temperature range under varying pressure conditions revealed that CH_4 selectivity increases as pressure is elevated from 1 to 30 bar.[28] ZnO/Al_2O_3 calcined to form $ZnAl_2O_4$ phase is the only catalyst in literature reported to exhibit complete CO selectivity from 400 to 700 °C at an elevated pressure of 5 atm as well as relatively little decline in performance over an extended run at 600−700 °C for 210 h.[29]

We recently reported that RWGS catalysts composed of alkali carbonates (M_2CO_3, M = Cs, K, Na) dispersed on common support materials are completely selective for CO at temperatures up to 500 °C and 10 bar at moderate space velocity and are tolerant to H_2S impurities commonly found in CO_2 sources.[30] Dispersion stabilizes M_2CO_3 in an a reactive, amorphous state that can activate H_2 without a transition metal. We hypothesized that the reaction proceeds via deporotonation of H_2 by carbonate to form a bicarbonate and a alkali metal hydride. This alkali hydride subsequently reacts with CO_2, producing a formate intermediate. Formate thermally decomposes to release CO and generates an alkali hydroxide. The cycle is completed by the recombination of hydroxide with a proton from the bicarbonate, producing water and regenerating the carbonate catalyst.[30] Here, we investigate the activity of alkali metal carbonates dispersed on γ-Al_2O_3 under more stringent conditions relevant to process development across the intermediate temperature regime. At a high gas hourly space velocity (GHSV) of 30,000 h^{-1} and 10 bar pressure, we show that these catalysts are highly active, reaching equilibrium-limited CO yield starting 550 °C and remain completely selective for CO up to 700 °C with no CH_4 or coke formation. We further investigate K_2CO_3/γ-Al_2O_3 and Na_2CO_3/γ-Al_2O_3 to demonstrate their stability for 100s of hours on stream at 525 °C and tolerance to CH_4 and C_3H_8 impurities.

2. RESULTS AND DISCUSSION

2.1. Catalyst Preparation and Characterization

Al_2O_3 was selected as the catalyst support because it is the most commonly used support material for industrial heterogeneous catalysts.[31] Dispersed carbonate catalysts were prepared from commercially available γ-Al_2O_3 pellets by incipient wetness impregnation with an aqueous carbonate solution followed by drying under vacuum at 150 °C. The loadings for the dried catalysts were 34 wt% Cs_2CO_3 (Cs_2CO_3/γ-Al_2O_3), 18 wt% K_2CO_3 (K_2CO_3/γ-Al_2O_3), and 14 wt% Na_2CO_3 (Na_2CO_3/γ-Al_2O_3), which correspond to the same molar loading of carbonate. Due to lower solubility of Li_2CO_3 in water, an aqueous lithium formate ($LiHCO_2$) solution was loaded onto the support by incipient wetness impregnation. The prepared sample was then calcined at 400 °C for 5 h to obtain 11 wt% Li_2CO_3 (Li_2CO_3/γ-Al_2O_3).

Freshly synthesized dispersed carbonate catalysts were characterized using scanning electron microscopy (SEM). No difference was observed in the morphology of the bare Al_2O_3 support compared to the loaded carbonate catalysts and energy-dispersive X-ray spectroscopy (EDX) elemental mapping showed a uniform dispersion of the alkali metals on the support (Figure 2a). The powder X-ray diffraction (PXRD) patterns of the materials exhibited peaks corresponding to γ-Al_2O_3 but no peaks for carbonate phases (Figure 2b). The Brunauer-Emmett-Teller specific surface area of the bare γ-Al_2O_3 was 250.6 m^2/g, which decreased to 170.8 and 190.0 m^2/g for K_2CO_3/γ-Al_2O_3 and Na_2CO_3/γ-Al_2O_3, respectively. Notably, when stored on a benchtop under ambient conditions for extended periods of time (weeks to months), alkali aluminum carbonate hydroxide phases ($MAlCO_3(OH)_2$) were observed by PXRD (Figure SI1), accompanied by needle-like structures observed by SEM (Figure SI2c and SI2e). Formation of these structures can be attributed to sorption of CO_2 from air in the presence of water.[32] Shelf stability of the
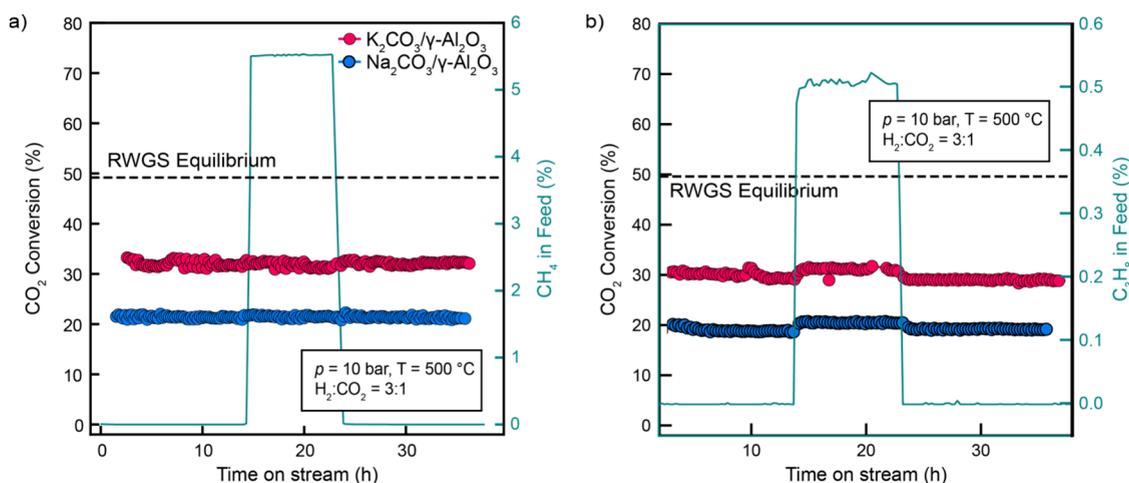
dispersed carbonate catalysts can be ensured by storing them under dry conditions.

2.2. Intermediate-Temperature RWGS Activity, Selectivity, and Stability

Testing RWGS activity under process-relevant conditions presents significant challenges in identifying a suitable reactor material, especially in lab-scale reactors where the ratio of reactor wall area to volume is high. The combination of CO_2 and H_2 at high temperature and pressure causes corrosion via metal dusting in common reactor materials such as stainless steel.[10] Corrosion-resistant alloys typically contain a high Ni content, which results in high background methanation and coking reactivity. Coatings can be applied to mitigate these problems by passivation of the reactor walls. We found that application of an amorphous Si coating (Silcolloy 2000 from SilcoTek) to an Incoloy reactor tube enabled RWGS experiments without substantial background interference at up to 700 °C at 1 bar pressure, but passivation was ineffective at >500 °C at 10 bar, for which large amounts of CH_4 and coke were produced. To measure catalyst activity at elevated temperature and pressure without interference from the reactor walls, a reactor was built using sintered silicon carbide (SiC) tubing (see S1.3).

RWGS activity was evaluated in the SiC reactor using ∼0.6 mL undiluted catalyst samples with a particle size of 177−250 μm. We first performed a temperature ramp from 400 to 700 °C holding at 50 °C intervals, with a 3:1 H_2:CO_2 gas mixture at 10 bar at a gas hourly space velocity (GHSV) of 30,000 h^{-1} (300 sccm). Each temperature step was maintained for 4 h to establish steady-state conversion and product gases were quantified every 13 min using a gas chromatograph (GC). Figure 2c and d show conversion and selectivity vs temperature. The background activity of the empty reactor (containing the inner quartz tube, quartz frit and quartz wool) without the catalyst was <1.5% throughout the temperature range. The bare γ-Al_2O_3 support itself catalyzes RWGS, although its activity fell well below the equilibrium limit even at 700 °C. The dispersed carbonate catalysts, on the other hand, are much more active, with Cs_2CO_3/γ-Al_2O_3 and K_2CO_3/γ-Al_2O_3 reaching equilibrium conversion at 550 °C, Na_2CO_3/γ-Al_2O_3 before 600 °C, and Li_2CO_3/γ-Al_2O_3 at 700 °C. All carbonate catalysts are completely selective for CO at all temperatures (Figure 2d). In the lower temperature range, where the catalysts exhibit subequilibrium conversions, the activity follows the order Cs > K ≫ Na ≫ Li, which follows the reverse order of charge density (C mm^{-3}): Cs^+ (6) < K^+ (11) < Na^+ (24) ≪ Li^+(98).[33] This inverse correlation between activity and cation charge density suggests that a lower cation charge density engenders a more basic and more reactive CO_3^{2-} that leads to faster turnover.

To assess their functional and structural stability, the catalysts were evaluated in 100 h runs at 540 °C with 10 bar of 3:1 H_2:CO_2 at 30,000 h^{-1} GHSV. Na- and K-based catalysts were selected for stability evaluation due to their abundance, favorable cost and relatively modest difference in catalytic performance as compared to Cs_2CO_3/γ-Al_2O_3. Under these conditions, both catalysts operate below the RWGS equilibrium limit, and therefore any deactivation should be clearly visible. As seen in Figure 2e, both K_2CO_3/γ-Al_2O_3 and Na_2CO_3/γ-Al_2O_3 exhibited stable CO_2 conversion and 100% selectivity for CO over the 100 h hold time. Analysis of the catalysts after the 100 h runs showed no observable changes in

Figure 3. Impurity tolerance: CO_2 conversion versus time on stream for dispersed carbonate catalysts before, during, and after exposure to a) 5.5% CH_4 and b) 0.5% C_3H_8 at 10 bar, 500 °C and 30,000 h^{-1} GHSV.

the morphology or alkali cation dispersion by SEM and EDX (Figure 2a). No discoloration of the catalysts was observed after the reaction, indicating the absence of coke deposition (Figure 2g and 2h). To quantify potential carbon deposits, we performed thermogravimetric analysis (TGA) on these samples under air to facilitate coke oxidation. As dispersed carbonates also decompose in this temperature range to release CO_2, TGA was performed under both N_2 and air, and the difference in weight loss between the two techniques was used to quantify carbon deposition (Figure SI3). The weight change profiles under N_2 and air matched closely for both samples, with no significant difference in weight loss, confirming that no coke was deposited on the catalysts during the 100 h on-stream period. The PXRD patterns of the post-reaction catalysts exhibit more intense γ-Al_2O_3 peaks as compared to the fresh catalyst, indicating increased crystallinity of Al_2O_3 as a result of the prolonged time at elevated temperature and steam pressure. However, no diffraction peaks corresponding to K_2CO_3 or Na_2CO_3 were observed, suggesting that alkali metal carbonates retain their amorphous and dispersed structure (Figure 2b). The BET specific surface areas post reaction were 150.5 and 143.8 m^2/g for K_2CO_3/γ-Al_2O_3 and Na_2CO_3/γ-Al_2O_3, respectively. The modest reductions in surface area post reaction are likely caused by partial sintering of the γ-Al_2O_3 support at the elevated temperatures of catalysis, because heating the bare support to 550 °C for 3 h resulted in a 20% reduction in its surface area (Table SI2).

Extended durability testing was performed at hte GmbH using a high-throughput unit featuring high-temperature metal alloy reactors equipped with ceramic inlay tubes to allow the operation at elevated pressures and ensure the inert behavior of the reactor walls (see S1.3). For these experiments, the catalyst pellets were ground and sieved to a size fraction of 160–250 μm and diluted 1:1 with SiC particles (200–300 μm) prior to loading into the reactor. The catalysts were held at 525 °C for 200 h with 3:1 H_2:CO_2 at 10 bar and 30,000 h^{-1} GHSV, and then the gas ratio was changed to 2:1 H_2:CO_2 for an additional 200 h. Operation at a 2:1 vs 3:1 H_2:CO_2 ratio may be desirable for some applications as it results in a lower H_2:CO ratio in the output stream. As seen in Figure 2f, both the K_2CO_3/γ-Al_2O_3 and Na_2CO_3/γ-Al_2O_3 showed good stability and essentially 100% selectivity for CO over the 400 h run time. Minimal background reactivity was observed for the SiC diluent. SEM

imaging and EDX mapping of K/Na post reaction revealed no changes in alkali metal dispersion or the morphology of the catalysts (Figure SI4). The presence of the diluent compromised further analysis of the spent K_2CO_3/γ-Al_2O_3 and Na_2CO_3/γ-Al_2O_3 catalyst samples for these experiments. Nonetheless, the activity, selectivity, and stability seen over 100s of hours at high space velocity and elevated pressure serves as a benchmark for intermediate-temperature RWGS.

The dispersed carbonate catalysts compare favorably with the previously reported $ZnAl_2O_4$ catalyst that was evaluated in a similar temperature regime at 5 bar. Whereas the $ZnAl_2O_4$ catalyst exhibited less than 20% CO_2 conversion at a space velocity of 15,000 $mL/g_{cat}/h$ at 550 °C at both 1 and 5 bar operating pressure, the K_2CO_3/γ-Al_2O_3 catalyst achieves equilibrium conversion at 550 °C at 10 bar with a space velocity of 60,000 $mL/g_{cat}/h$.[29,34]

2.3. Tolerance to Hydrocarbon Impurities

Tolerance to hydrocarbons is an important consideration for integration of RWGS with FT. Since typical FT reactors operate at 40–70% conversion,[21] the off-gas that remains after product separation contains significant amount of H_2, CO_2, CO, and light hydrocarbon gases (methane to propane). Depending on the process design, it may be necessary to recycle the reactant gases through the RWGS unit[35] to achieve optimal overall efficiency. In high temperature units, the hydrocarbon impurities can be reformed in situ. At intermediate temperature, however, this pathway is not viable and hydrocarbons could cause catalyst fouling by coking.[36] Tolerance to hydrocarbons would therefore simplify the process design by avoiding the need to separate them from the reactant gases in the recycle loop. To this end, we evaluated the effect of the addition of either 5% CH_4 or 0.5% C_3H_8 to the input gas feed on the dispersed carbonate catalysts. A baseline activity was established for 12 h, then the hydrocarbon impurity was introduced into the feed for 8 h, and finally the conditions were returned to the impurity-free baseline for an additional 12 h. As seen in Figure 3, both K_2CO_3/γ-Al_2O_3 and Na_2CO_3/γ-Al_2O_3 were unperturbed by the addition of either CH_4 or C_3H_8, maintaining 100% CO selectivity and very similar activity. The slight increase in the CO_2 conversion upon introduction of C_3H_8 resulted from a slightly higher H_2:CO_2 ratio in the gas mixture tank used to provide this impurity (see S1.3). Additionally, no coke

deposition was observed on the catalyst samples post reaction. The inertness to CH_4 and C_3H_8 shown here, combined with our previous demonstration of H_2S tolerance,[30] suggest dispersed carbonate catalysts may have substantially broader impurity tolerance compared to conventional transition metal-based catalysts.

2.4. Shaped Catalysts

While catalyst powders (<250 μm particle size) are useful for probing intrinsic activity, larger catalyst particles with well-defined morphology are necessary for practical reactor designs. As an initial assessment of activity in a form factor suitable for larger reactors, we evaluated 18 wt% K_2CO_3 dispersed on the intact 3 mm γ-Al_2O_3 pellets from which the powders were prepared. To accommodate the larger particles, we assembled a 1" OD stainless steel reactor coated with amorphous Si, which was capable of operating under RWGS conditions at 10 bar and up to 550 °C without interference from the reactor walls. The pellet K_2CO_3/γ-Al_2O_3 catalyst was evaluated with 3:1 H_2:CO_2 at 10 bar and a GHSV of 3,200 h^{-1} in a temperature ramp from 425 to 550 °C (with 25 °C steps) and then held at 450 °C for 140 h. The CO_2 conversion was stable and the CO selectivity remained at 100% over the entire 140 h on stream (Figure 4).
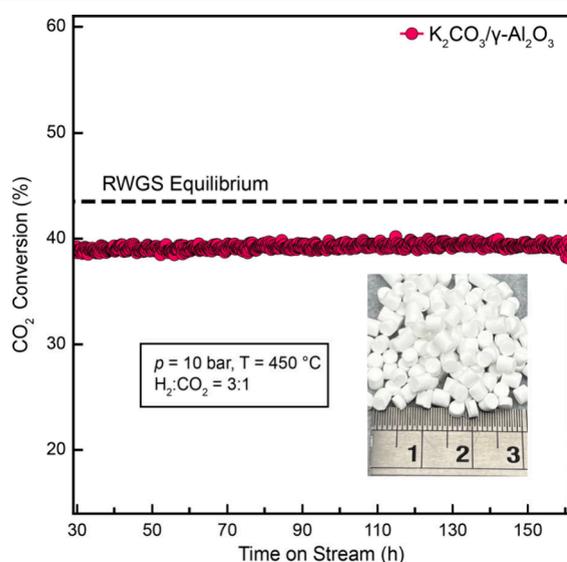
Figure 4. Shaped catalyst: CO_2 conversion versus time on stream for 18 wt% K_2CO_3/γ-Al_2O_3 pellets for a 140 h hold at 450 °C, 10 bar, and 3,200 h^{-1} GHSV.

3. CONCLUSION

The production of renewable syngas to decarbonize fuels and chemicals hinges on improving and scaling RWGS catalysis. The results above show that dispersed carbonates are a compelling option for intermediate temperature RWGS, which may be easier to scale and integrate in PtL processes than conventional high-temperature processes. While more stress testing is needed, dispersed carbonates manifest a solution to the formidable selectivity challenge for RWGS when methanation and coking are thermodynamically favored, highlighting an advantage of hydrogenation catalysis in the absence of transition metals. The low cost of the catalyst components and the ease of preparing dispersed carbonate

catalysts, requiring only a loading step and no redox pretreatment, simplifies the path to scale up.

◼ ASSOCIATED CONTENT

Ⓢ Supporting Information

The Supporting Information is available free of charge at https://pubs.acs.org/doi/10.1021/jacsau.5c00127.

Additional experimental details, methods, and characterization of catalyst materials, including SEM images, EDX maps, XRD spectra, TGA data, and N_2 sorption characterization (PDF)

◼ AUTHOR INFORMATION

Corresponding Author

Matthew W. Kanan — *Stanford University, Stanford, California 94305, United States;* ⓘ orcid.org/0000-0002-5932-6289; Email: mkanan@stanford.edu

Authors

Kesha N. Tamakuwala — *Stanford University, Stanford, California 94305, United States*
Robert P. Kennedy — *Stanford University, Stanford, California 94305, United States*
Chastity S. Li — *Stanford University, Stanford, California 94305, United States;* ⓘ orcid.org/0000-0001-7576-8362
Benjamin Mutz — *hte GmbH, 69123 Heidelberg, Germany*
Peter Boller — *hte GmbH, 69123 Heidelberg, Germany*
Simon R. Bare — *SSRL, SLAC National Accelerator Laboratory, Menlo Park, California 94025, United States;* ⓘ orcid.org/0000-0002-4932-0342

Complete contact information is available at:
https://pubs.acs.org/10.1021/jacsau.5c00127

Notes

◼ ACKNOWLEDGMENTS

◼ REFERENCES

(1) Thor Wismann, S.; Larsen, K.-E.; Mølgaard Mortensen, P. Electrical Reverse Shift: Sustainable CO2 Valorization for Industrial Scale. *Angew. Chem., Int. Ed.* **2022**, *61*, No. e202109696.

(2) Vázquez, F. V.; Koponen, J.; Ruuskanen, V.; Bajamundi, C.; Kosonen, A.; Simell, P.; Ahola, J.; Frilund, C.; Elfving, J.; Reinikainen, M.; Heikkinen, N.; Kauppinen, J.; Piermartini, P. Power-to-X technology using renewable electricity and carbon dioxide from ambient air: SOLETAIR proof-of-concept and improved process concept. *Journal of CO₂ Utilization* **2018**, *28*, 235−246.

(3) Claxton, H. A.; James, A.; Mckenna, M. J.; Ticehurst, P. R. PCT WO2022079407A1: Process for synthesising hydrocarbons. 2022;

https://patents.google.com/patent/WO2022079407A1/en?q=(syngas)&inventor=Paul+Ticehurst&oq=Paul+Ticehurst+syngas.

(4) Schuetzle, R.; Schuetzle, D.; Wright, H.; Hanbury, O.; Caldwell, M. PCT WO2021225642A1: Reverse water gas shift catalytic reactor systems. 2021; https://patents.google.com/patent/WO2021225643A1/en?oq=WO2021225643.

(5) Schultz, M. A.; Obern, J.; Simpson, S. D. US Patent US8,809,015B2: Methods and systems for the production of hydrocarbon products. 2014; https://patents.google.com/patent/US8809015B2/en?oq=US8809015B2.

(6) Jeswani, H. K.; Chilvers, A.; Azapagic, A. Environmental sustainability of biofuels: a review. *Proc. R. Soc. A.* **2020**, *476*, No. 20200351.

(7) Outlook for Energy; ExxonMobil, 2022. Accessed: 2022-04-30.

(8) Bierhals, J. *Ullmann's Encyclopedia of Industrial Chemistry*; John Wiley Sons, Ltd., 2001.

(9) Tarifa, P.; Ramirez Reina, T.; González-Castaño, M.; Arellano-García, H. Catalytic Upgrading of Biomass-Gasification Mixtures Using Ni-Fe/MgAl2O4 as a Bifunctional Catalyst. *Energy Fuels* **2022**, *36*, 8267−8273.

(10) Rostrup-Nielsen, J.; Christiansen, L. J. *Concepts in Syngas Manufacture*; Imperial College Press, 2011.

(11) Busca, G.; Spennati, E.; Riani, P.; Garbarino, G. Mechanistic and Compositional Aspects of Industrial Catalysts for Selective CO_2 Hydrogenation Processes. *Catalysts* **2024**, *14*, 95.

(12) Yang, L.; Pastor-Pérez, L.; Villora-Pico, J.; Gu, S.; Sepúlveda-Escribano, A.; Reina, T. CO_2 valorisation via reverse water-gas shift reaction using promoted Fe/CeO2-Al2O3 catalysts: Showcasing the potential of advanced catalysts to explore new processes design. *Applied Catalysis A: General* **2020**, *593*, No. 117442.

(13) Almeida Benalcázar, E.; Noorman, H.; Maciel Filho, R.; Posada, J. A. Decarbonizing ethanol production via gas fermentation: Impact of the $CO/H_2/CO_2$ mix source on greenhouse gas emissions and production costs. *Comput. Chem. Eng.* **2022**, *159*, No. 107670.

(14) Álvarez Galván, C.; Schumann, J.; Behrens, M.; Fierro, J. L. G.; Schlögl, R.; Frei, E. Reverse water-gas shift reaction at the Cu/ZnO interface: Influence of the Cu/Zn ratio on structure-activity correlations. *Applied Catalysis B: Environmental* **2016**, *195*, 104−111.

(15) Twigg, M. V.; Spencer, M. S. Deactivation of supported copper metal catalysts for hydrogenation reactions. *Applied Catalysis A: General* **2001**, *212*, 161−174. Catalyst Deactivation.

(16) Chen, C.-H.; Chen, H.-K.; Huang, W.-H.; Chen, C.-L.; Choojun, K.; Sooknoi, T.; Tian, H.-K.; Lin, Y.-C. Reversal of methanation-oriented to RWGS-oriented Ni/SiO2 catalysts by the exsolution of Ni2+ confined in silicalite-1. *Green Chem.* **2023**, *25*, 7582−7597.

(17) Lin, Y.-C.; Rajagopal, S.; Chou, P.-T.; Peng, P.-Y.; Lu, Y.-R.; Chen, C.-L.; Tsai, M.-H.; Wang, C.-H. Crafting a Methanation-Resistant, Reverse Water−Gas Shift-Active Nickel Catalyst with Significant Nanoparticle Dimensions Using the Molten Salt Approach. *ACS Sustainable Chem. Eng.* **2024**, *12*, 14771−14783.

(18) Hancke, R.; Holm, T.; Ulleberg, Øy. The case for high-pressure PEM water elec- trolysis. *Energy Conversion and Management* **2022**, *261*, No. 115642.

(19) Gupta, M.; Spivey, J. J. In *New and Future Developments in Catalysis*; Suib, S. L., Ed.; Elsevier: Amsterdam, 2013; pp 87−126.

(20) Van Hecke, W.; Bockrath, R.; De Wever, H. Effects of moderately elevated pressure on gas fermentation processes. *Bioresour. Technol.* **2019**, *293*, No. 122129.

(21) Adelung, S.; Maier, S.; Dietrich, R.-U. Impact of the reverse water-gas shift operating conditions on the Power-to-Liquid process efficiency. *Sustainable Energy Technologies and Assessments* **2021**, *43*, No. 100897.

(22) Lu, B.; Kawamoto, K. Preparation of mesoporous CeO2 and monodispersed NiO particles in CeO2, and enhanced selectivity of NiO/CeO2 for reverse water gas shift reaction. *Mater. Res. Bull.* **2014**, *53*, 70−78.

(23) Zhang, Q.; Bown, M.; Pastor-Pérez, L.; Duyar, M. S.; Reina, T. R. CO_2 Conversion via Reverse Water Gas Shift Reaction Using Fully

Selective Mo−P Multicomponent Catalysts. *Ind. Eng. Chem. Res.* **2022**, *61*, 12857−12865.

(24) Pajares, A.; Prats, H.; Romero, A.; Viñes, F.; de la Piscina, P. R.; Sayós, R.; Homs, N.; Illas, F. Critical effect of carbon vacancies on the reverse water gas shift reaction over vanadium carbide catalysts. *Applied Catalysis B: Environmental* **2020**, *267*, No. 118719.

(25) Zhang, Q.; Pastor-Pérez, L.; Jin, W.; Gu, S.; Reina, T. Understanding the promoter effect of Cu and Cs over highly effective -Mo2C catalysts for the reverse water-gas shift reaction. *Applied Catalysis B: Environmental* **2019**, *244*, 889−898.

(26) Ahmadi Khoshooei, M.; Wang, X.; Vitale, G.; Formalik, F.; Kirlikovali, K. O.; Snurr, R. Q.; Pereira-Almao, P.; Farha, O. K. An active, stable cubic molybdenum carbide catalyst for the high-temperature reverse water-gas shift reaction. *Science* **2024**, *384*, 540−546.

(27) Juneau, M.; Vonglis, M.; Hartvigsen, J.; Frost, L.; Bayerl, D.; Dixit, M.; Mpourm- pakis, G.; Morse, J. R.; Baldwin, J. W.; Willauer, H. D.; Porosoff, M. D. Assessing the viability of K-Mo2C for reverse water−gas shift scale-up: molecular to laboratory to pilot scale. *Energy Environ. Sci.* **2020**, *13*, 2524−2539.

(28) Vidal Vázquez, F.; Pfeifer, P.; Lehtonen, J.; Piermartini, P.; Simell, P.; Alopaeus, V. Catalyst Screening and Kinetic Modeling for CO Production by High Pressure and Temperature Reverse Water Gas Shift for Fischer−Tropsch Applications. *Ind. Eng. Chem. Res.* **2017**, *56*, 13262−13272.

(29) Joo, O.-S.; Jung, K.-D. Stability of ZnAl2O4 catalyst for reverse-water-gas-shift reac-tion (RWGSR). *Bulletin of the Korean Chemical Society* **2003**, *24*, 86−90.

(30) Li, C. S.; Frankhouser, A. D.; Kanan, M. W. Carbonate-catalyzed reverse water-gas shift to produce gas fermentation feedstocks for renewable liquid fuel synthesis. *Cell Reports Physical Science* **2022**, *3*, No. 101021.

(31) Trueba, M.; Trasatti, S. P. -Alumina as a Support for Catalysts: A Review of Fundamental Aspects. *Eur. J. Inorg. Chem.* **2005**, *2005*, 3393−3403.

(32) Veselovskaya, J. V.; Derevschikov, V. S.; Kardash, T. Y.; Stonkus, O. A.; Tru- bitsina, T. A.; Okunev, A. G. Direct CO_2 capture from ambient air using K2CO3/Al2O3 composite sorbent. *International Journal of Greenhouse Gas Control* **2013**, *17*, 332−340.

(33) Rayner-Canham, G.; Overton, T. *Descriptive Inorganic Chemistry*; W.H. Freeman and Company, 2009.

(34) Park, S.-W.; Joo, O.-S.; Jung, K.-D.; Kim, H.; Han, S.-H. Development of ZnO/Al2O3 catalyst for reverse-water-gas-shift reaction of CAMERE (carbon dioxide hydrogenation to form methanol via a reverse-water-gas-shift reaction) process. *Applied Catalysis A: General* **2001**, *211*, 81−90.

(35) Hannula, I.; Kaisalo, N.; Simell, P. Preparation of Synthesis Gas from CO_2 for Fis- cher−Tropsch Synthesis—Comparison of Alternative Process Configurations. *C J. Carbon Res.* **2020**, *6*, 55.

(36) de Vasconcelos, S. M.; Meira de Souza, A. E. A.; Santos Araujo, M.; Moraes Silva, M. A.; Dantas Araujo, F. A.; de Lima Filho, N. M.; Moraes de Abreu, C. A. Effect of the Light Alkane Content of Natural Gas on the Production of Hydrogen and Coke During the Dry Reform. *Journal of Advanced Chemical Engineering* **2019**, *9*, 191.

■ NOTE ADDED AFTER ASAP PUBLICATION

This Letter published ASAP on March 12, 2025. Due to production error, eqs 2 and 4 have been updated and the corrected version reposted on March 24, 2025.